Opto-Electronic Advances

Supplementary information

January 2024, Vol. 7, No. 1

DOI: 10.29026/oea.2024.230121

Multi-dimensional multiplexing optical secret sharing framework with cascaded liquid crystal holograms

Keyao Li[1,2,†], Yiming Wang[3,†], Dapu Pi[1], Baoli Li[1], Haitao Luan[1], Xinyuan Fang[1*], Peng Chen[3*], Yanqing Lu[3] and Min Gu[1]

[1]Institute of Photonic Chips, University of Shanghai for Science and Technology, Shanghai 200093, China; [2]Centre for Artificial-Intelligence Nanophotonics, School of Optical-Electrical and Computer Engineering, University of Shanghai for Science and Technology, Shanghai 200093, China; [3]National Laboratory of Solid State Microstructures, and College of Engineering and Applied Sciences, Nanjing University, Nanjing 210093, China.

[†]These authors contributed equally to this work.

*Correspondence: XY Fang, E-mail: xinyuan.fang@usst.edu.cn; P Chen, E-mail: chenpeng@nju.edu.cn

This file includes:

Supplementary information for this paper is available at https://doi.org/10.29026/oea.2024.230121

Section 1: The influence of the number of multiplexed channels on reconstructive image quality

The loss function is composed of mean square error (MSE) of each image in each multiplexed channel, which can be expressed as:

$$\text{Loss} = \sum_{l=1}^{k} L_{\text{MSE}}^{l} \ , \tag{S1}$$

$$L_{\text{MSE}} = \frac{1}{mn} \sum_{i=1}^{m} \sum_{j=1}^{n} [O(i,j) - G(i,j)]^2 \ , \tag{S2}$$

$$PSNR = 10\log_{10}\left(\frac{255^2}{L_{\text{MSE}}}\right) \ , \tag{S3}$$

where k is the number of the multiplexed channels in our optical secret sharing scheme. m and n represent the pixel number of images. $O(i,j)$ and $G(i,j)$ represent the pixel value of holographic reconstruction and ground truth. The peak signal-to-noise ratio (PSNR) is calculated in Eq. (S3). The multiple mean square error (MSE) values of the output and the ground truth result in the loss function of the network. To illustrate the relationship between the PSNR of the reconstructive images and the multiplexed channels, we calculated the maximum, average and minimum PSNR values of multiplexed channels, as shown in the Fig. S2. The digital images of letter from A-J were selected for multiplexing. In line with the optical sharing scheme in our manuscript, the dimension of circular polarizations with different spacing distances between two shares were utilized for multiplexing. As can be seen, the increase of the multiplexing channels leads to the deterioration of the overall reconstruction qualities.

Section 2: The crack difficulty of the optical secret sharing framework

In the proposed optical secret sharing framework, the authentication information only can be decrypted with correct decryption keys. To simulate the information cracking scene of the framework, one LC hologram is fixed, then the relation of image quality with the effective pixel number of the other LC hologram is obtained. In addition to these effective pixels, the other phase distributions the LC hologram was set as 0. As shown in Fig. S6, the PSNR of the comprehensive image quality increases from 13.37 dB to 15.49 dB. Without losing generality, the multiplication image ("×") was selected to visual display the process, which illustrates the necessity of two holograms with enough pixels.

Section 3: Optical secret sharing framework with three shares

To increase the multiplexing channel numbers, we theoretically proposed a multidimensional multiplexing optical secret sharing framework containing three secret shares. As shown in the Fig. S7(a), the three shares successively placed along the direction of the input light (z-axis). Each share has an effective size of 2.12 mm×2.12 mm, which contains 256×256 pixels. The initial distances from share 1 to share 2 and share 3 are selected as d_{12} =1 cm, d_{13}=2 cm, respectively. And the observing plane is 5 cm apart from share 1. To illustrate the multiplexing scheme, share 2 and share 3 can also be moved 1cm in the z direction from the initial places. Also, the physical dimension of circular polarizations is employed for multiplexing. In this context, 17 multiplexed holographic images displayed in Fig. S7(c) can be obtained through this proposed optical secret sharing framework with three shares in Fig. S7(b).

Section 4: Optical secret sharing with circular and linear polarization states multiplexing.

The orthogonal linear polarization states can be used to increase the information channels of this holographic secret sharing scheme. Without losing generality, here four channel holographic multiplexing images with two LC holograms is illustrated to prove the concept.

Specifically, due to the property of controllable diffraction efficiency, the voltage of the first layer LC hologram should be set at the "on-state", which leads to a high diffraction efficiency. Meanwhile, for circular-polarized or linear-polarized incident beams, the voltage of the second layer LC hologram should be set either at the "on-state" or "half-on-state", respectively. It is worthwhile mentioning that the LC device with "half-on-state" corresponds to 50% of the peak

diffraction efficiency. Here, four polarization conversion processes are listed below. After considering the coherent and incoherent interferences in output beams, the multiplexing hologram can be designed as shown in the first two phase images in the upper row of Fig.S8 ($e^{i\varphi_1}$ and $e^{i\varphi_2}$). Then the other four images are expected to be reconstructed by light beams with different polarization states.

1. $LCP \rightarrow e^{-i\pi/2}RCPe^{i\varphi_1} \rightarrow e^{-i\pi}LCPe^{i\varphi_1}e^{-i\varphi_2}$,
2. $RCP \rightarrow e^{-i\pi/2}LCPe^{-i\varphi_1} \rightarrow e^{-i\pi}RCPe^{-i\varphi_1}e^{i\varphi_2}$,
3. $LCP + RCP \rightarrow e^{-i\pi/2}RCPe^{i\varphi_1} + e^{-i\pi/2}LCPe^{-i\varphi_1}$
$\rightarrow 1/\sqrt{2}[e^{-i\pi/2}RCPe^{i\varphi_1} + e^{-i\pi}LCPe^{i\varphi_1}e^{-i\varphi_2}] + 1/\sqrt{2}[e^{-i\pi/2}LCPe^{-i\varphi_1} + e^{-i\pi}RCPe^{-i\varphi_1}e^{i\varphi_2}]$,
4. $LCP - RCP \rightarrow e^{-i\pi/2}RCPe^{i\varphi_1} - e^{-i\pi/2}LCPe^{-i\varphi_1}$
$\rightarrow 1/\sqrt{2}[e^{-i\pi/2}RCPe^{i\varphi_1} + e^{-i\pi}LCPe^{i\varphi_1}e^{-i\varphi_2}] - 1/\sqrt{2}[e^{-i\pi/2}LCPe^{-i\varphi_1} + e^{-i\pi}RCPe^{-i\varphi_1}e^{i\varphi_2}]$,

here, the symbol of $\rightarrow$ denotes a modulation of incident light beams by one layer of LC hologram, wherein the phase distributions of $e^{\pm i\varphi_1}$ and $e^{\pm i\varphi_2}$ can be provided for left (+) and right (−) circularly polarized components, respectively. Also, an additional phase retardation of $e^{-i\pi/2}$ appears.

Supplementary figures

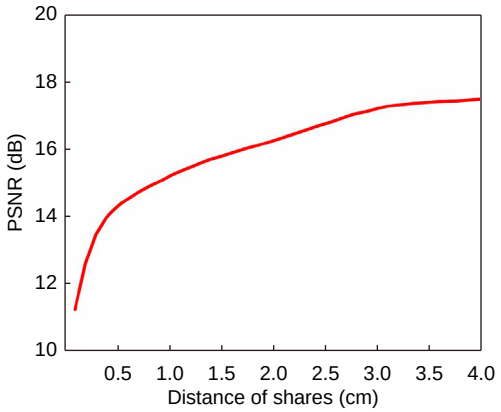

Fig. S1 | The relationship of the two circular-polarization-multiplexing images' quality with the distance between two LC holograms.

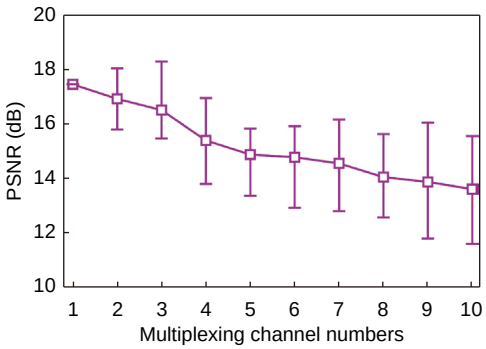

Fig. S2 | The relationship of PSNR values with multiplexed channel numbers. The symbol of error bar represents the maximum, average and minimum PSNR values of multiplexed images.

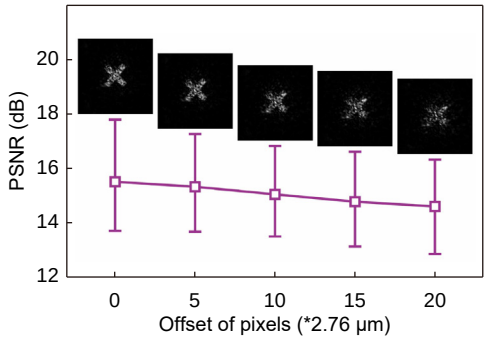

Fig. S3 | The effect of the pixel offset on reconstruction images' quality.

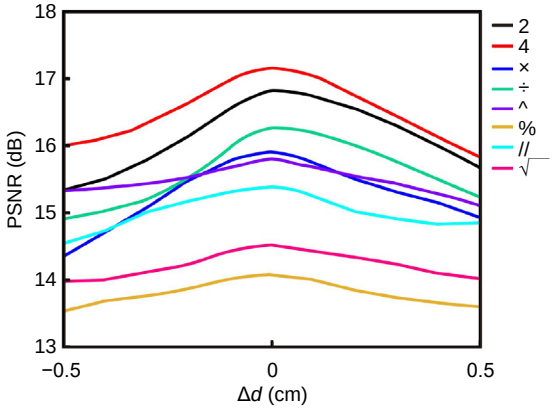

Fig. S4 | Sensitivity of distance mismatch between two LC holograms. Δ*d* denotes deviation along the light propagation direction.

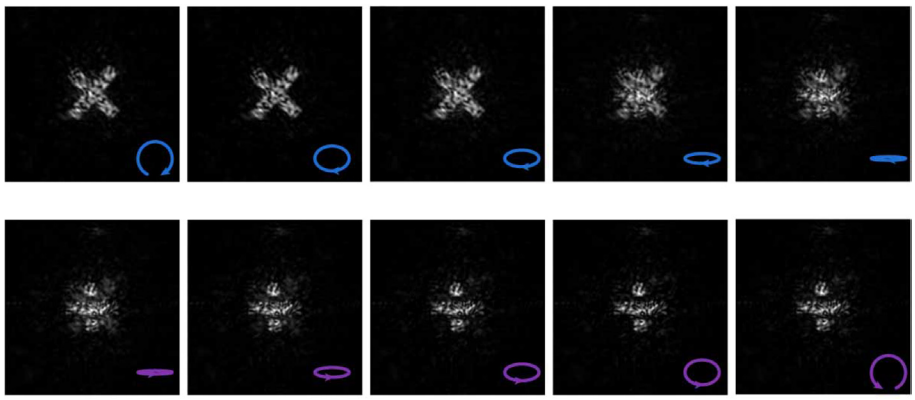

Fig. S5 | The images reconstructed by different elliptically-polarized beams.

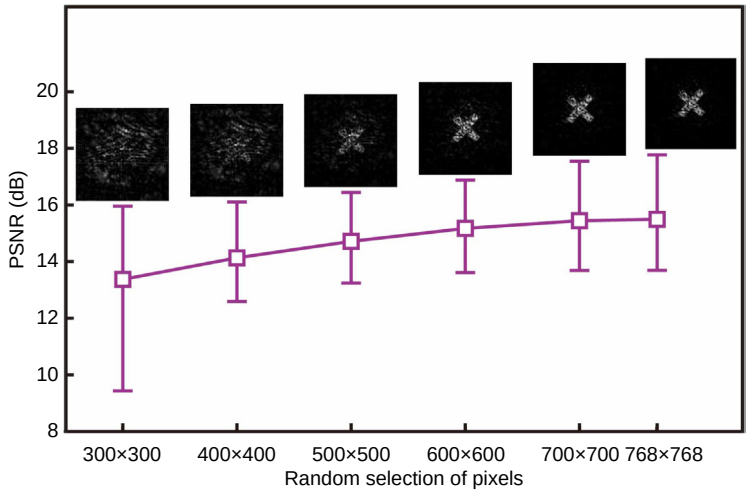

Fig. S6 | The PSNR values of cascaded holograms with different effective pixel number.

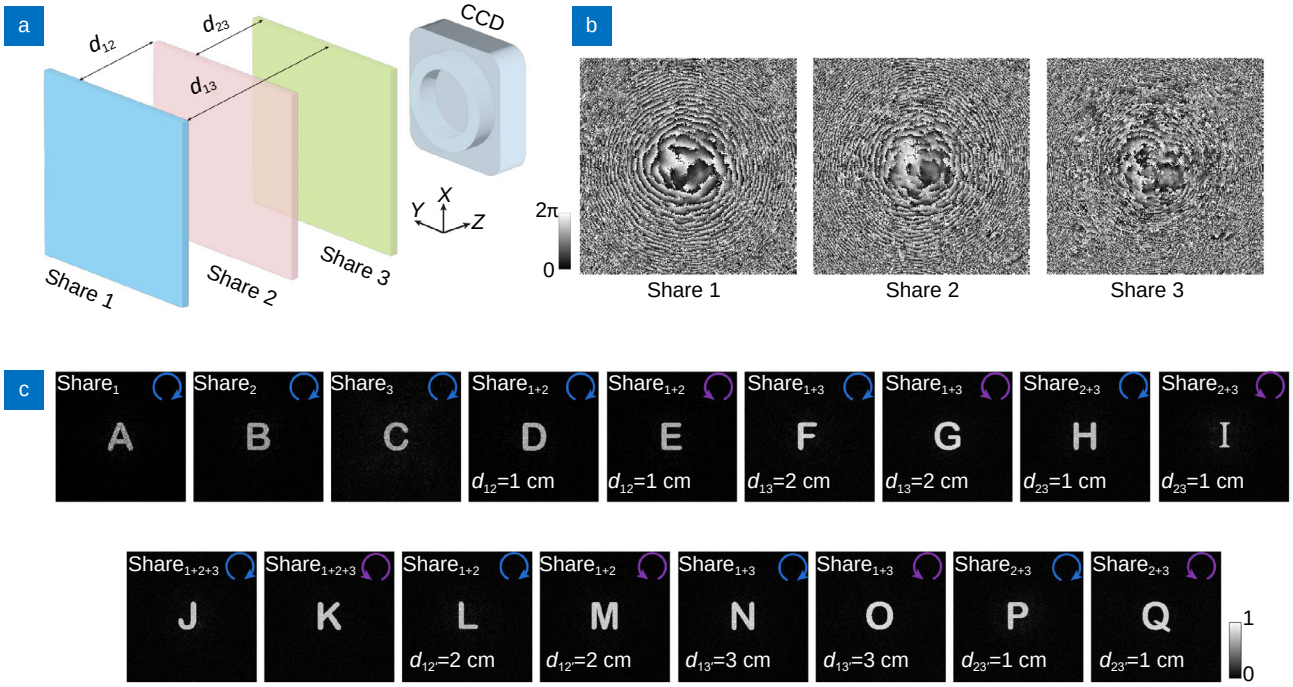

Fig. S7 | The illustration of multidimensional multiplexing optical secret sharing framework with three secret shares. (**a**) Schematic diagram of three secret shares framework. d_{ij} represents the distance between share *i* and share *j*. (**b**) The phase distributions of three secret shares. (**c**) The decryption keys and corresponding decrypted images.

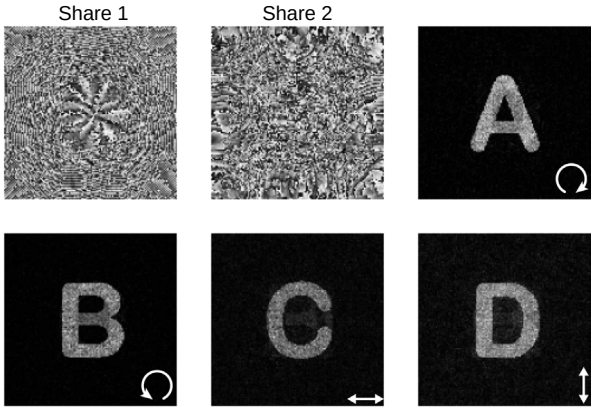

Fig. S8 | Illustration of the linear and circular polarization multiplexed secret sharing framework.